A COMPLETE PFC INDUCTOR DESIGN FOR LIGHTING EQUIPMENT APPLICATIONS

Wai Keung Mo[1] , Kasper M.Paasch[2], Thomas Ebel[3]
Centre for Industrial Electronics
Department of Mechanical and Electrical Engineering
University of Southern Denmark
Alsion 2, 6400
Sønderborg, Denmark
Tel.: +45 /65507627[1], +45/65501695[2], +45/65501288[3],
E-mail: wkmo@sdu.dk[1], Paasch@sdu.dk[2], ebel@sdu.dk[3]
URL: https://www.sdu.dk/da

Acknowledgements

This work was supported by Syddansk Vækstforum, the Bitten and Mads Clausen Foundation, the European Regional Development Fund as well as Interreg Deutschland-Danmark with funds from the European Regional Development Fund via the PE: Region and the PE-Region Platform projects. Find further information on Interreg Deutschland-Denmark on www.interreg5a.eu.

Keywords

«Active filter », «Boost», «Harmonics», «Magnetic device», «Simulation» «Winding topology»

Abstract

This paper presents the comparison of two novel air-gap inductor designs: two step air-gap solution (TSAG) and curved air gap solution (CAG). The effective mathematical inductance model of the proposal CAG design is derived and verified experimentally in terms of harmonic and EMI emissions. A complete optimal PFC inductor design procedure is given.

Introduction

Table 1: Definition of symbols used

Symbol	unit	definition	Symbol	unit	definition
$L_{req(min)}$	H	Minimum inductance for PFC inductor solution	ΔI	A	Ripple current
η		Converter efficiency	I_{av}	A	DC average current
$V_{in(min)}$	V	RMS minimum line voltage	P_o	W	Output power
k		$k = \frac{\Delta I}{I_{av}}$	L_{eff}	H	Effective inductance
f_s	Hz	Operation frequency	TSAG		Two step air gap inductor
CCM		Continuous conduction mode	I_{pk}	A	Peak excitation current
DCM		Discontinuous conduction mode	CAG		Curved-air gap inductor
D		Duty cycle	PFC		Power factor correction

Although LED lighting equipment with dimming function is used widely in many nations because of high reliability and high energy efficiency, it is a great challenge to satisfy Class C, published in IEC 61000-3-2 [1], regarding harmonic current regulation. Furthermore, the worst harmonic situation might not be in the maximum loading conditions or full dimming. Hence, the PFC solution [2],[3], boost pre-regulator, must be operated in CCM not only to improve the harmonic content but also to reduce the significant conduction loss because of I_{pk}. However, there are several drawbacks. Firstly, it is difficult

to sustain a high-power factor when the output power has gradually decreased because of DCM operation in light loading. Secondly, the boost inductor requires an air gap to prevent core saturation, which results in extra-winding loss.

Practical PFC inductor considerations

The minimum inductance for CCM PFC booster converter, $L_{req(min)}$, is given by

$$L_{req(min)} = \frac{\sqrt{2}V_{in(\min)}D}{\Delta I f_s}[4] \quad (1)$$

The ΔI at the peak of the $V_{in(min)}$ is stated by

$$\Delta I = \frac{k\sqrt{2}P_o}{\eta V_{in(min)(1+\frac{k}{2})}} \quad (2)$$

Substituting (2) into (1), it can be rewritten

$$L_{req}(\min) \geq \frac{\eta D(1+\frac{k}{2})V_{in}^2(\min)}{k f_s P_o} \quad (3)$$

The desired inductance for the CCM PFC converter must be larger than $L_{req(min)}$ given by equation (3). The $L_{req(min)}$ is inversely proportional to P_o implying two practical solutions to satisfy the harmonic requirements: 1. Large P_o (no dimming) demands on small $L_{req(min)}$ which means small inductor size. 2. Small P_o (100% dimming) demands on the large $L_{req(min)}$ which means large inductor volume. Although many PFC inductor solutions can be reduced size by an increase of fs and ΔI, the drawbacks result in large winding loss and significant EMI issues. Hence, a variable inductor concept based on a magnetic structure with novel air gap design is introduced.

In contrast to the recent publications, only few research papers focus on development of the inductance mathematical model with air-gap parameters to design an appropriate PFC inductor for satisfying harmonic and conducted emission limits. The TSAG and CAG analysis are given in section II. The inductance mathematical model of CAG is presented in section IV. Implementation of CAG in the CCM PFC boost converter and design procedure are provided in section IV, the L_{eff} equation of the CAG is examined to be applicable in the economical PFC boost inductor design in terms of D and f_s as well as different air gap dimension. In section VI, experimental verification is provided to verify the harmonic current and EMI emission.

Variable air gap inductor

TSAG

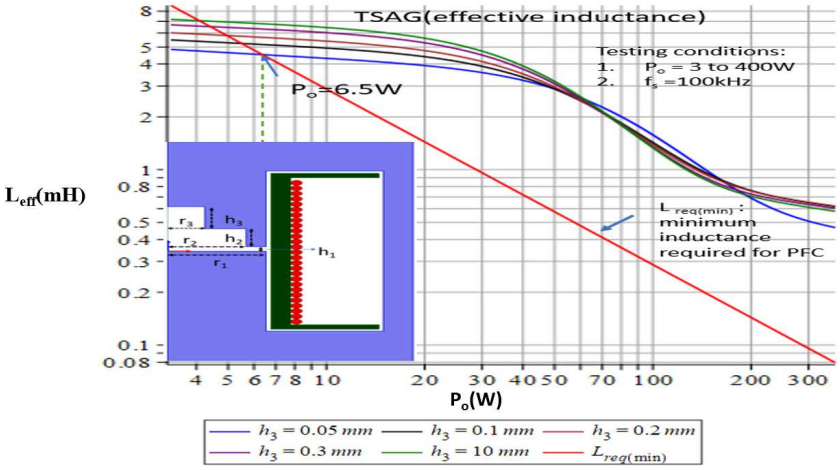

Fig 1: Choosing L_{eff} for PFC requirements by TSAG

Fig.1 illustrates the L_{eff} as a function of P_o with different h_3. Inspection of these curves, representing the

L_{eff}, shows that there is a region where L_{eff} is inversely proportional to P_o and the initial L_{eff} is proportional to h_3. At ($4W \leq P_o \leq 60W$), this region commences, but, for ($60W < P_o < 200W$), the green curve is lower than other curves. Finally, the purple curve is larger than other curves when $200W < P_o < 300W$. The red line represents the $L_{req(min)}$ for PFC solution, all the curves above this red line satisfy $L_{req(min)}$ with given air gap parameter (h_3). Hence, the minimum P_o is 6.5W for given TSAG solution [5] to fulfill $L_{req(min)}$ illustrated in fig.1.

CAG

Fig.2 illustrates L_{eff} as a function of P_o with different air gap parameter c. Inspection of these curves, representing L_{eff}, shows that there is a region where L_{eff} is inversely proportional to P_o and the initial L_{eff} is proportional to c.

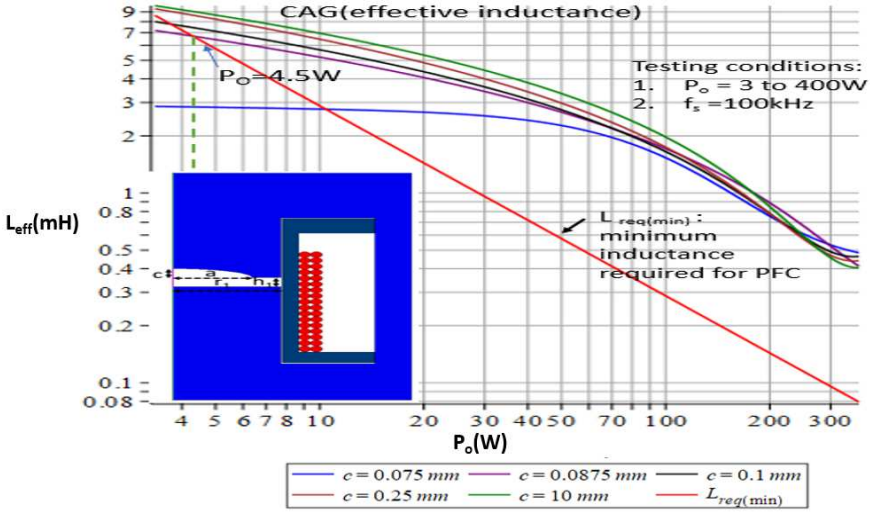

Fig.2: Choosing L_{eff} for PFC requirements by CAG

At ($4W \leq P_o \leq 200W$), this region commences, but, for ($200W < P_o < 300W$), the green curve is above than the other curves, it has gradually decreased to 0.4mH and is lower than other at P_o=340W. The red line represents the $L_{req(min)}$ for PFC solution, all the curves above this line satisfy $L_{req(min)}$ with given air gap parameter c. Hence, the minimum P_o is 4.5W except the blue curve for given CAG solution [6] illustrated in fig.2.

Result comparison between TSAG and CAG

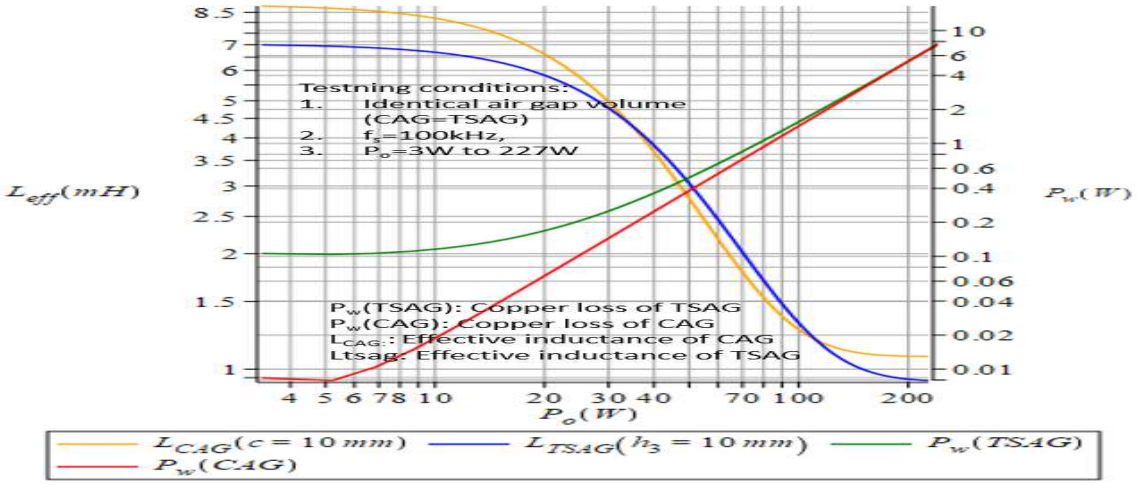

Fig.3: L_{eff} and copper loss (P_w) comparison between TSAG and CAG

Fig.3 illustrates the L_{eff} comparison between TSAG and CAG under identical test conditions, initial L_{eff} (CAG) is 28.5% larger than L_{eff} (TSAG), the L_{eff} difference has dramatically reduced at ($4W < P_o < 30W$) and lower than 5% at ($30W < P_o < 120W$), however, L_{eff} (CAG) is 10% larger than L_{eff} (TSAG) at ($120W<P_o<227W$). Apart from this, initial P_w (CAG), copper loss of CAG, is 90% smaller than P_w (TSAG) (copper loss of TSAG) and the copper loss difference has significantly reduced at $P_o > 100W$. Fig.4 shows the core loss comparison between TSAG and CAG, the loss difference has gradually increased for $4W < Po < 227W$.

Finally, the P_c (CAG) is 5% lower than P_c (TSAG) at Po=227W. Hence, the technical issues of TSAG are increased losses (P_c+P_w) and its initial L_{eff} is 30% lower than the CAG at $P_o \leq 4W$ with identical air gap parameters and test conditions.

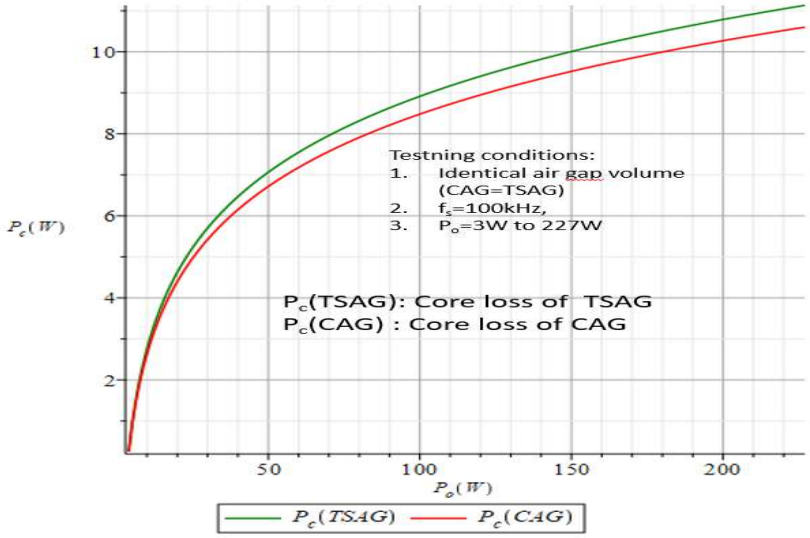

Fig.4: Core loss (P_c) comparison between TSAG and CAG

Consequently, the CAG is an optimal air gap solution to minimize the inductor volume and increase the overall PFC efficiency as well as lower harmonic regardless of loading conditions.

Analytical CAG inductance model

An innovative approach of CAG consists of the curved air gap (CAG1) and a small portion of standard air gap (minor gap) illustrated in fig.5, because this minor gap can extend its L_{eff} and maximize L_{eff} with high P_o capability shown in fig.13. The CAG1 works as a progressively accumulated air reluctance to provide large inductance at small P_o because of less core saturation and small inductance at large P_o because of large core saturation.

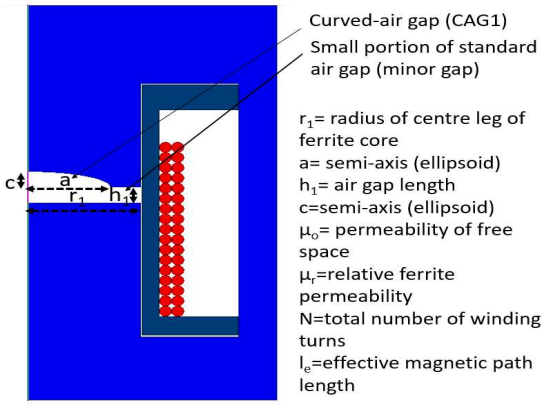

Fig. 5: Curved air gap inductor with air gap dimensions

The equivalent magnetic circuit of the CAG and its reluctance model is shown in fig.6 with n-individual reluctances ϑ_{fi}, which consists of the curved air gap reluctance R_g in series with the curved magnetic core reluctance R_m, to be connected in parallel with each other. Hence, the initial CAG inductance is

$$L_o \approx \frac{N^2}{R_c+\frac{1}{\sum_{i=1}^{n}\frac{1}{\vartheta_{fi}}}} \approx \frac{N^2}{(R_c+\frac{1}{\sum_{i=1}^{n}\left(\frac{1}{(R_{gi}+R_{mi})}\right)})} \approx \frac{N^2\mu_r\mu_o\pi {r_1}^2}{h_1\mu_r+l_e-h_1-c+\sum_{i=2}^{n-2}\frac{\frac{c}{(n-1)}}{1-(\frac{1}{r_1}(a-\frac{c(i-2)}{(n-1)})^2}} \quad (4)$$

where $R_c=\frac{l_{eff}-(c-h_1)}{\mu_r\mu_o\pi r_1^2}$, $R_{gc}=\frac{h_1}{\mu_o\pi r_1^2}$, $R_{gi}=\frac{h_i}{\mu_o\pi r_i^2}$, $R_{mi}=\frac{h_i}{\mu_o\pi(r_1^2-r_i^2)}$ and $a=\sum_{i=1}^{n} r_i$

All the equation parameters are given in fig.5 and 6.

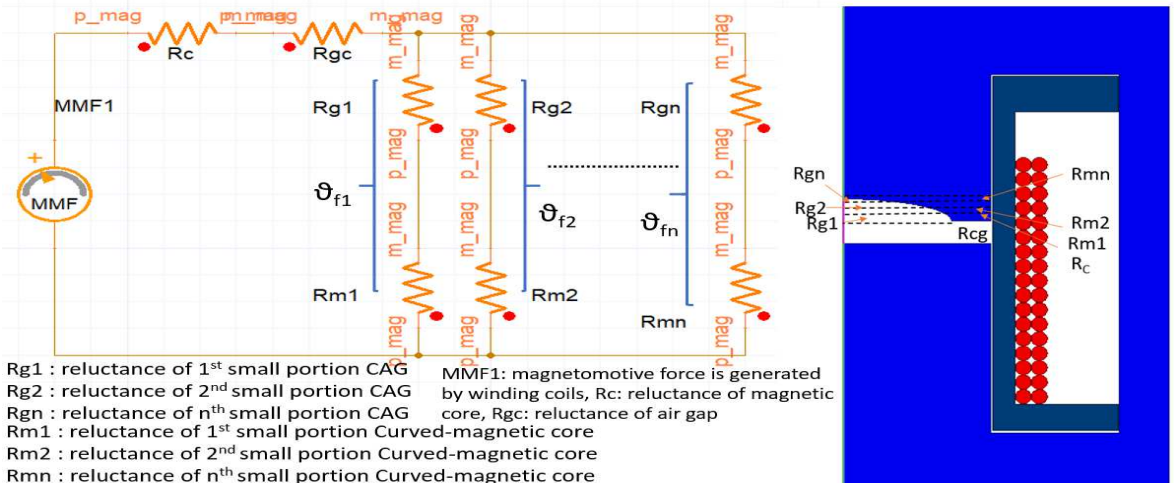

Fig.6: Equivalent magnetic circuit of the CAG inductor and reluctance model

Effective inductance mathematical model

The voltage across an inductor is related to its flux linkage and this in turn is related to the current, the dependence of the inductance on its current must be considered.

$$V=\frac{d(Li)}{dt}=\left(L_o+\frac{dL}{dI}I\right)\frac{di}{dt}=L_{eff}\frac{dI}{dt} \quad (5)$$

$$L_{eff}=L_o+\frac{dL}{dI}I_{pk} \quad (6)$$

where $I_{pk}=\frac{\sqrt{2}P_o}{\eta V_{in(min)}}$

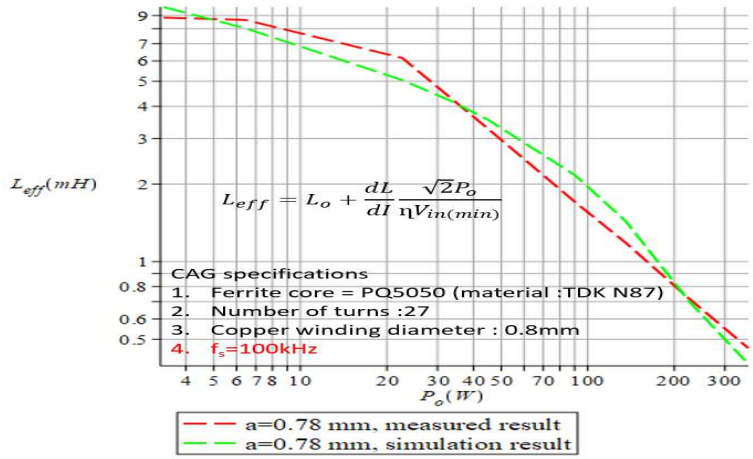

Fig. 7: L_{eff} (CAG) comparison between measured and mathematical simulation results (a=0.78mm)

Substituting of (4) and $\gamma = \frac{dL}{dI} = -\frac{(b\alpha \cosh\frac{\alpha x}{\delta} + \rho\varphi \sinh\frac{\varphi x}{\delta} \sinh \alpha x\delta)}{\delta sinh^2 \alpha\delta x cosh^2\frac{\varphi x}{\delta}}$ into (6), it can be written as

$$L_{eff} = \frac{N^2\mu_r\mu_o\pi r^2}{h_1\mu_r + l_e - h_1 - c + \sum_{i=2}^{n-2}\frac{\frac{c}{(n-1)}}{1-(\frac{1}{r_1}(a-\frac{c(i-2)}{(n-1)})^2}} - \frac{(b\alpha \cosh\frac{\alpha x}{\delta} + \rho\varphi \sinh\frac{\varphi x}{\delta} \sinh \alpha x\delta)}{\delta sinh^2 \alpha\delta x cosh^2\frac{\varphi x}{\delta}} x \quad (7)$$

where $x = \frac{\sqrt{2}P_o}{\eta V_{in(min)}}$, α, β, δ, φ are air-gap geometrical parameters.

Figs 7 and 8 illustrate the L_{eff} comparison against P_o by the air gap parameters (a & c). The differences between measured and simulation results, given in fig.7, are 13 %@a=0.78mm at (3W < P_o < 35W) and 10% @a=0.78mm at (35W < P_o < 200W). Comparing the simulation and measured L_{eff} against P_o, shown in fig.8, less 5% @c=0.075mm at (4W <P_o < 250W) and 10% @c=0.0875mm at (20W <P_o < 60W) as well as 15%@c=0.0875mm at (60W <P_o < 200W), is also promising and validates the L_{eff} mathematical model and its analysis. Although there are minor errors between them, the L_{eff} mathematical models [7] are sufficient to predict L_{eff} behavior against P_o.

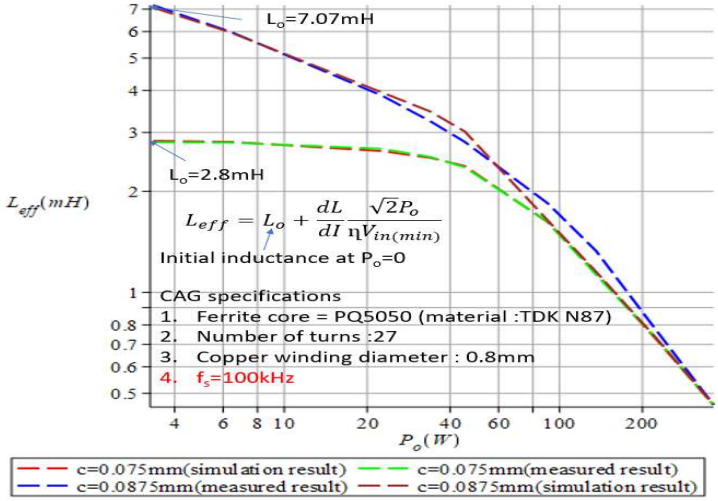

Fig.8: L_{eff} (CAG) comparison between measured and mathematical simulation results (c=0.075mm & 0.0875mm)

Implementation of CAG in the CCM PFC Boost converter and design procedure

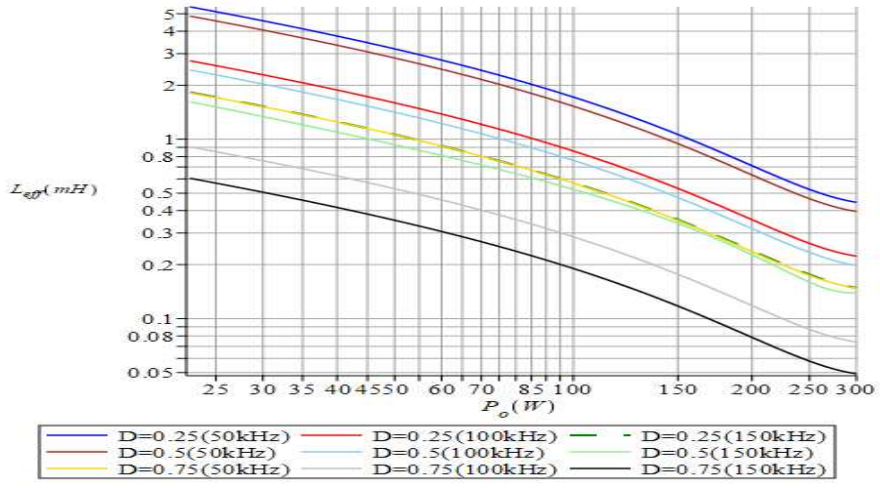

Fig. 9: L_{eff} with 3 duty cycles (D=0.25, 0.5 and 0.75) and 3 operation frequency (fs=50kHz,100kHz, 150kHz) against P_o

Fig.9 examines the L_{eff} of CAG with given conditions against the P_o and its design procedure is shown as follows.

1. Calculate the minimum inductance for sustaining boost converter in CCM operation by equation (3)
2. Determine the CAG air gap parameters by equation (4)
3. Determine the appropriately effective inductance from fig.9 with given operation conditions. E.g., DT=0.25, f=100kHz, P_o =300W, L_{eff}= 0.2mH

Fig.10 presents a complete optimal CAG inductance design algorithm [8] to optimize the winding loss by k and the effective inductance for satisfying harmonic requirements.

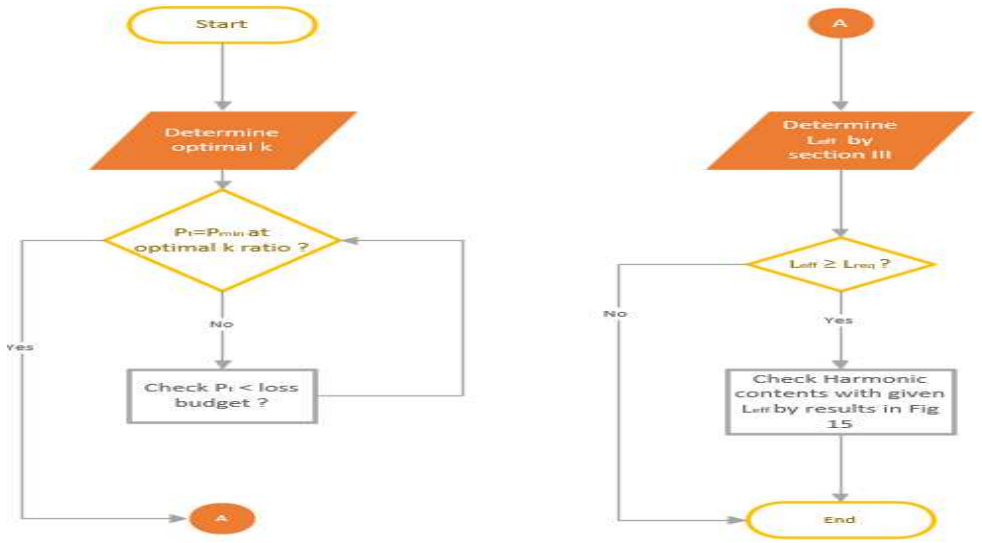

Fig. 10 Optimal CAG inductance design algorithm

Experimental results and measurement set-up

Experimental measurement set-up

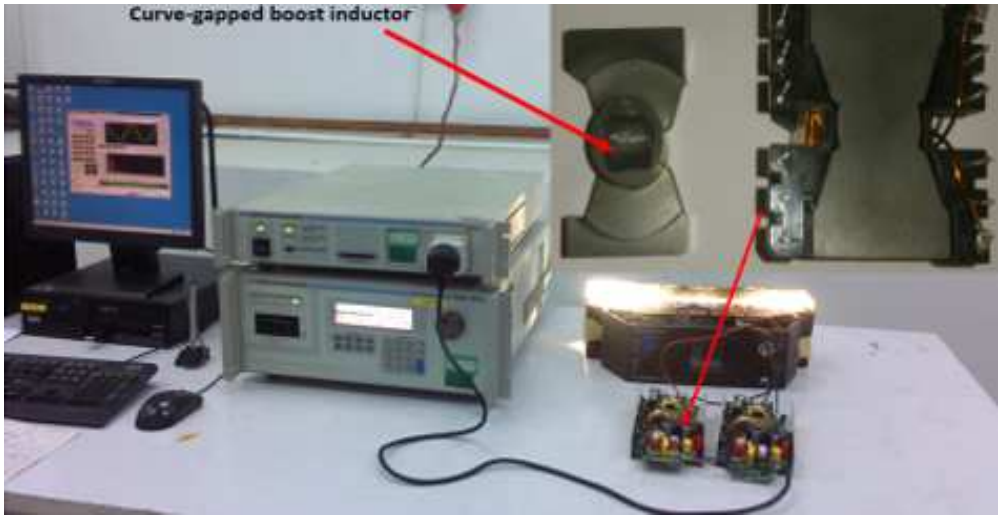

. Fig,11: Harmonic current measurement set-up

To verify the proposed CAG solution, several prototypes were built and test with PFC converter (UC3854) as well as full bridge converter (UCC22980) for operation of 200 LED lighting equipment shown in fig.11.

The specifications of the prototypes are shown in Table 2.

Table 2 : The specification of the entire system prototype

The specifications of the PFC boost converter	The specifications of the full bridge converter
1.Vin: 230Vrms /50Hz 2. Vo 385 V(dc) 3. Po: 300W 4. f_s:100 kHz 5.CAG: 6mH (initial inductance) 6. PFC controller: UC3854	1.Vin: 385V(dc) 2. V_o: 12V(dc) 3. P_o: 270W 4. f_s:200kHz 5. PWM controller: UCC22980
The specification of LED	The specifications of the CAG
CREE J series 2016 (V_f= 2.9V to 3.1V@ I_{fmax}=150mA)	1.Ferrite core = PQ 5050 (material: TDK N87), 2. Number of turns: 27 3. Copper winding diameter: 0.8mm

Experimental results

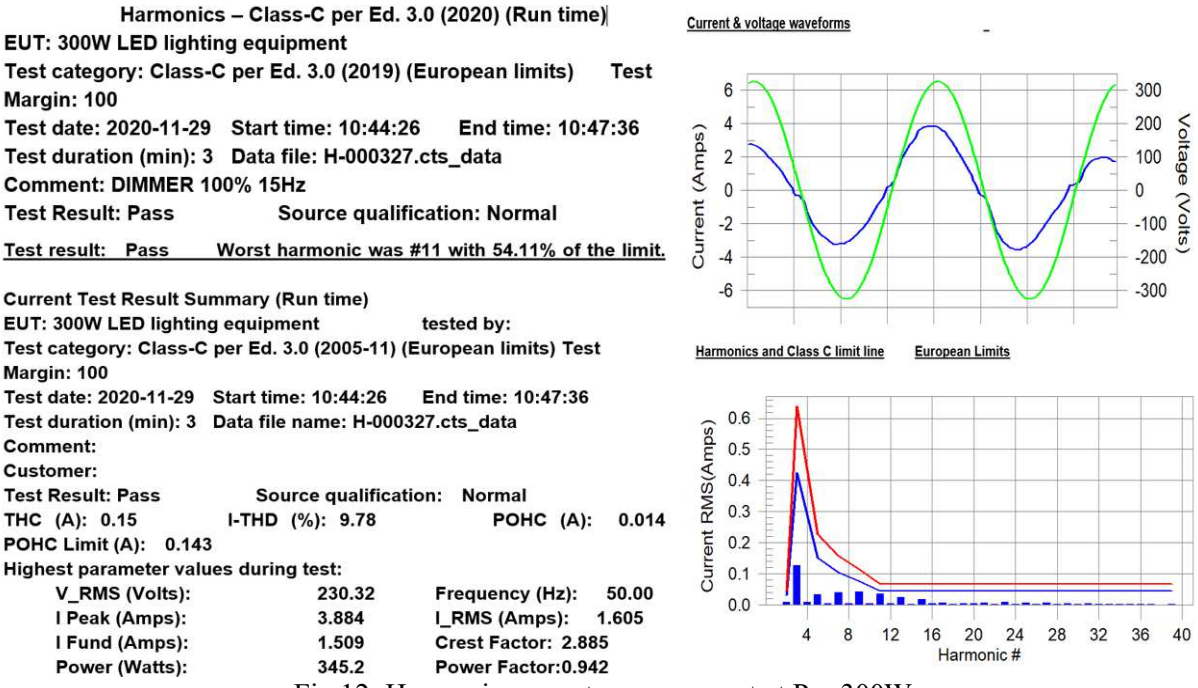

Fig.12: Harmonic current measurement at Po=300W

The harmonic result at P_o=300W with LED lighting application is shown in Fig.12. The blue and red curve represent 100% and 150% over the harmonic limit, the worst harmonic is 11th (550Hz) and 55.4% of the Class C limit.

Result comparison between CAG with and without minor gap solution

The result comparison between CAG with and without minor gap solution against P_o addresses the L_{eff} and EMI emission shown in fig.13, 14 and 15. Under identical testing conditions, the initial L_{eff} of CAG (no minor gap) is 75% larger than CAG (minor gap); however, this L_{eff} has been significantly reduced to 0.2mH ,which is one sixth of CAG (minor gap), at 35W < P_o < 90W and is below $L_{req(min)}$ at 90W < Po < 340W illustrated in fig.13, hence, this solution is inappropriate for PFC inductor design. The comparison reveals that the L_{eff} of CAG with minor gap is a better solution to sustain sufficient L_{eff} over $L_{req(min)}$ to satisfy the harmonic requirement.

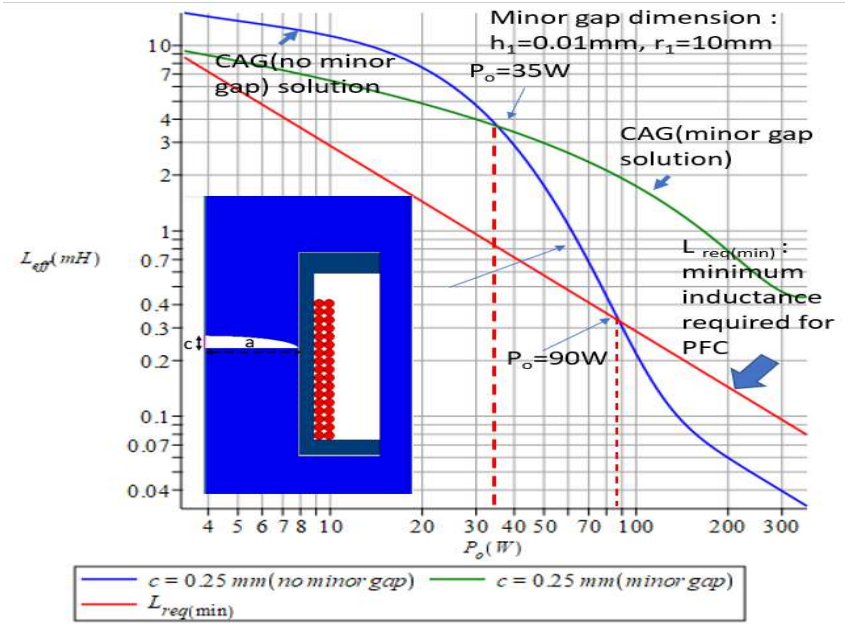

Fig.13: L_{eff} comparison between CAG (with and without minor gap solution given identical testing conditions) against P_o

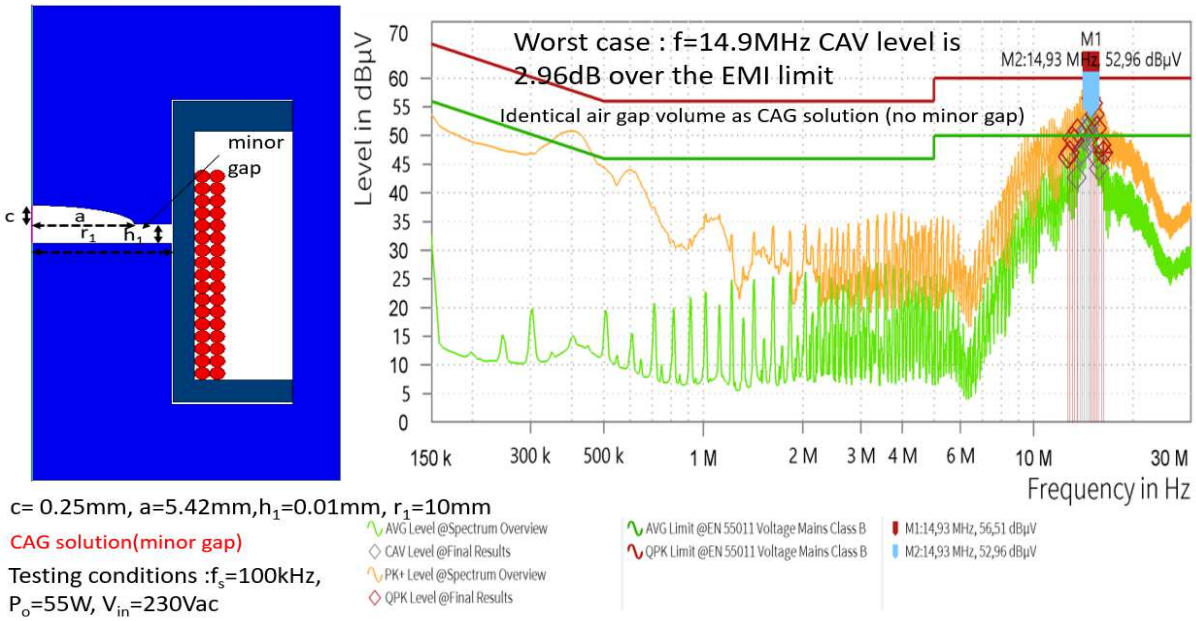

c= 0.25mm, a=5.42mm,h_1=0.01mm, r_1=10mm

CAG solution(minor gap)

Testing conditions :f_s=100kHz, P_o=55W, V_{in}=230Vac

Fig.14: Conducted emission with CAG minor gap solution (air gap dimension: c=0.25mm, a=3.86 mm, h_1=0.01mm, r_1=10mm)

The prototypes of the CAG with and without minor gap solution together with the whole LED lighting system are measured on a R&S ESR EMI receiver under identical testing conditions (P_o=55W, fs=100kHz, V_{in}=230V). The test results indicate the highest peak of conducted emission level (53 dBµV shown in fig.14 (CAG with minor gap)) and (74.9dBµV shown in fig.15 (CAG without minor gap)) at 14.9MHz, which should be considered for the PFC inductor design. Hence, the result comparisons reveal that the CAG with optimal minor gap can improve the harmonic content and have compared EMI performance.

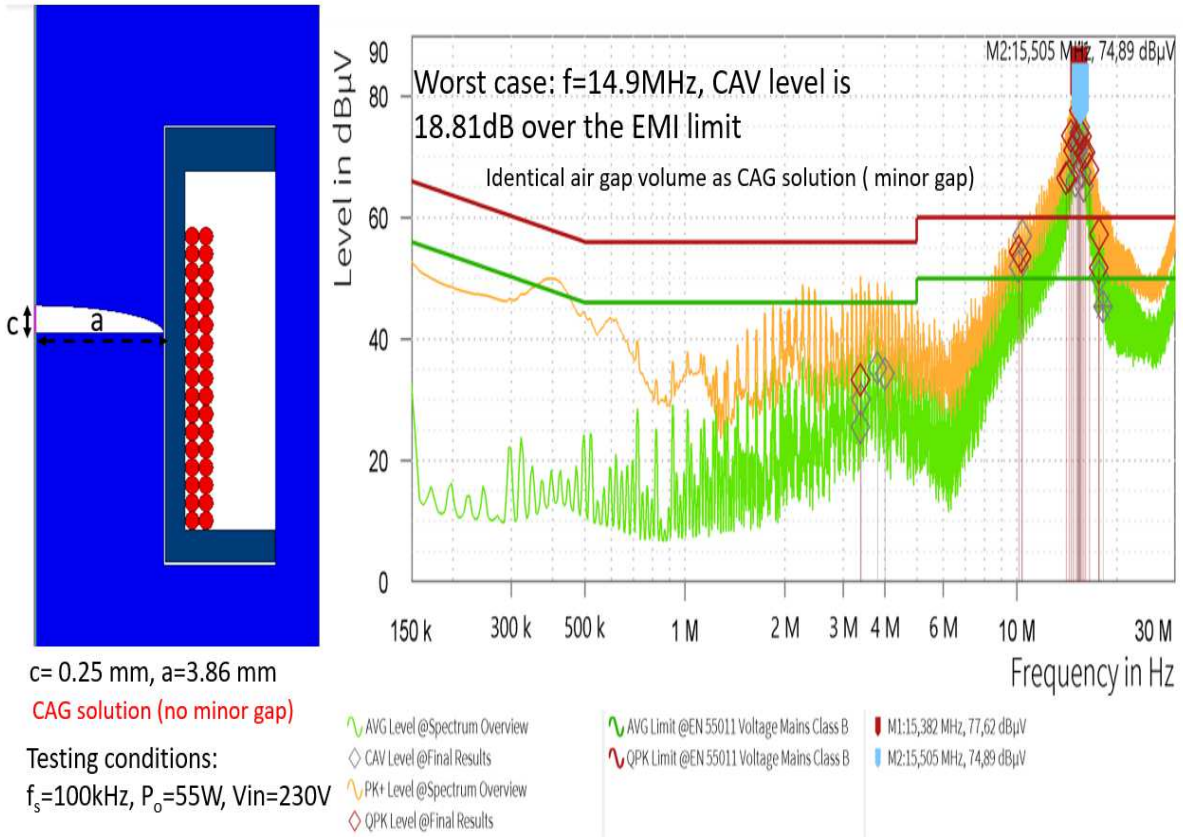

Fig.15: Conducted emission with CAG no minor gap solution (air gap dimension: c=0.25mm, a=5.47mm)

Conclusion

The presented new concept of the curved air-gap inductor is a key solution to improve the harmonic content regardless of loading conditions and minimizing inductor volume. Given L_{eff}-P_o curves of the CAG solution against duty cycle and operation frequencies shown in fig.9 together with equation (7), the optimal CAG dimension can be determined effectively. Comparison of EMI measurement shows that the CAG with optimal minor gap structure is a preferrable solution to minimize conducted emission.

References

[1]. IEC, EN61000-3-2:2019, EMC-Part3-2: Limits for harmonic current emission (equipment input current ≤ 16A per phase)

[2]. Jee-Woo Lim and Bong Hwart-Kwon, "A power factor controller for single-stage PWM rectifiers," IEEE Trans. Ind.Electron., vol.46, pp.1035-1037, Oct.1999

[3]. R.Redl,L.Balogh,and N.O.Sokal, " A new family of single-stage isolated power-factor correctors with fast regulation of the output voltage," Rec. IEEE PESC, pp 1137-1144, 1994.

[4]. Philip C. Too, "UC3854 controlled Power Factor," Unitrode application note U-134

[5]. W.G. Hurley, "Power factor correction for ac/dc converters with cost effective inductive filtering," in Proc. IEEE 31st Power Electron. Spec. Conf. (PESC'00), vol.1, Galway, Ireland, June 2000 pp332-337.

[6]. Wai Keung Mo, Kasper M.Paasch and Thomas Ebel, " Optimal gapped boost inductor design for power factor correction applications," EPE 2021 23rd European Conference on Power Electronics and Applications , p.1-11.

[7]. E. Stenglein and M. Albach, "Analytical calculation method for the non-linear characteristic of ferrite-cored inductors with stepped air gap," Springer, Electr Eng (2017) 99: 421-429.

[8]. W.K.Mo, Kasper M Paasch and Thomas Ebel, " Improved method of power inductor design with DC current impact," IEEE 14th international conference on compatibility , power electronics and power engineering, pp120-126, 2020.